

Hurricane Forecasting: A Novel Multimodal Machine Learning Framework

LÉONARD BOUSSIOUX*

Operations Research Center, Massachusetts Institute of Technology, Cambridge, MA, USA
leobix@mit.edu

CYNTHIA ZENG*

Operations Research Center, Massachusetts Institute of Technology, Cambridge, MA, USA
czeng12@mit.edu

THÉO GUÉNAIS

School of Engineering and Applied Sciences, Harvard University, Cambridge, MA, USA
tguenais@fas.harvard.edu

DIMITRIS BERTSIMAS[†]

Sloan School of Management and Operations Research Center, Massachusetts Institute of Technology, Cambridge, MA, USA
dbertsim@mit.edu

ABSTRACT

This paper describes a machine learning (ML) framework for tropical cyclone intensity and track forecasting, combining multiple distinct ML techniques and utilizing diverse data sources. Our framework, which we refer to as Hurricast (HURR), is built upon the combination of distinct data processing techniques using gradient-boosted trees and novel encoder-decoder architectures, including CNN, GRU and Transformers components. We propose a deep-feature extractor methodology to mix spatial-temporal data with statistical data efficiently. Our multimodal framework unleashes the potential of making forecasts based on a wide range of data sources, including historical storm data, and visual data such as reanalysis atmospheric images. We evaluate our models with current operational forecasts in North Atlantic and Eastern Pacific basins on 2016-2019 for 24-hour lead time, and show our models consistently outperform statistical-dynamical models and compete with the best dynamical models, while computing forecasts in seconds. Furthermore, the inclusion of Hurricast into an operational forecast consensus model leads to a significant improvement of 5% - 15% over NHC's official forecast, thus highlighting the complementary properties with existing approaches. In summary, our work demonstrates that combining different data sources and distinct machine learning methodologies can lead to superior tropical cyclone forecasting. We hope that this work opens the door for further use of machine learning in meteorological forecasting.

Significance statement. Machine learning techniques have not been fully explored for improving tropical cyclone movement and intensity changes. This work shows how the use of advanced machine learning techniques combined with routinely available information can be used to efficiently improve 24-h tropical cyclone forecasts. The successes demonstrated for 24-h forecasts provide a recipe for improving for longer leads, further reducing forecast uncertainties and benefiting society.

1. Introduction

A tropical cyclone (TC) is a low-pressure system originating from tropical or subtropical waters and developing by drawing energy from the sea. It is characterized by a

warm core, organized deep convection and a closed surface wind circulation about a well-defined center. Every year, tropical cyclones cause hundreds of deaths and billions of dollars of damage to households and businesses (Grinsted et al. 2019). Moreover, there is growing evidence suggesting consistent hurricane intensity escalation due to climate change, leading to potentially greater damaging power (Knutson et al. 2019). Therefore, producing an accurate prediction for TC track and intensity with sufficient lead time is critical to undertake life-saving measures.

The forecasting task encompasses the track, intensity, size, structure of TCs, and associated storm surges, rainfall, and tornadoes. Most forecasting models focus on producing track (trajectory) forecasting and intensity forecasting, i.e., intensity measures such as the maximum sustained wind speed in a particular time interval. Current operational TC forecasts can be classified into dynamical

*Equal contribution

[†]Corresponding author: Dimitris Bertsimas, dbertsim@mit.edu

models, statistical models and statistical-dynamical models (Rhome 2007). Dynamical models, also known as numerical models, utilize powerful supercomputers to simulate atmospheric fields' evolution using sophisticated physically-motivated dynamical equations. Statistical models approximate historical relationships between storm behavior and storm-specific features, and typically do not explicitly consider the physical process. Statistical-dynamical models use statistical techniques but further includes atmospheric variables provided by dynamical models. Lastly, ensemble models, also known as consensus forecasts, combine the forecasts made by individual models or multiple runs of a single model.

This paper introduces a machine learning framework, referred to as Hurricast (HURR), for both intensity and track forecasting by combining multiple machine learning approaches and several data sources. Our contributions are four-fold:

1. We present a new multimodal¹ machine learning methodology for TC intensity and track predictions by combining distinct forecasting methodologies to utilize multiple individual data sources. We demonstrate improvement in prediction accuracy by combining efficiently statistical features based on historical data and spatial-temporal features extracted from atmospheric reanalysis maps.
2. We demonstrate that our machine learning approach using XGBoost (Chen and Guestrin 2016), a boosted-tree-based method, with advanced processing techniques, such as feature extraction from computer vision and deep learning, can outperform operational statistical-dynamical models and compete with dynamical models. Our tree-based methodology is particularly useful for combining data sources.
3. We introduce an encoder-decoder model, based on a Convolutional Neural Network (LeCun et al. 1989) encoder and a Gated Recurrent Unit (Chung et al. 2014) or Transformer (Vaswani et al. 2017) decoder, that can perform TC spatial-temporal feature extraction from statistical and spatial-temporal data. To the best of our knowledge, this is the first time a deep learning architecture is explicitly compared to operational forecasts for TC track and intensity forecast at the same time. This is also the first time the success of a Transformer architecture is demonstrated in TC prediction.
4. Based on our testing, ensemble models that include our machine learning model as an input can outperform all current operational models. This demonstrates the potential value of developing machine

learning approaches as a new branch methodology for hurricane forecasting.

The paper is structured as follows: Section 2 outlines the current state of forecasting methods in the discipline; Section 3 describes the data used in the scope of this study; Section 4 elucidates the key challenges; Section 5 explains detailed methodologies to resolve these challenges, as well as the operational principles underlying our Machine Learning models; Section 6 describes the experiments conducted; Section 7 deals with conclusions from the results and validates the effectiveness of our framework. Finally, Section 8 discusses future work and guidance for real-world deployment of our Hurricast approach.

2. Related Work

a. Dynamical Methods

Dynamical models, also known as numerical models, are complex and computationally expensive numerical simulations. Forecasts are made by solving physical equations that model atmospheric dynamics using initial conditions based on observations, measures and geographical knowledge of the area. Dynamical models can be global or coarse resolution, and mesoscale or fine resolution, but the former will not be able to resolve high intensities. One major weakness of dynamical models is that errors or uncertainties around initialization grow as time evolves in the simulation, leading to increasingly inaccurate longer-time predictions. They also struggle with physical processes (precipitation, microphysics, radiation) that are typically parameterized. Moreover, their computational time is often a bottleneck to obtain near real-time forecasts, especially when reactivity is at stake. As a result, dynamical methods typically take several hours to run and can only be updated several times daily, thus they cannot utilize the most recent data and have to provide real-time guidance through interpolation.

The European Center for Medium-Range Weather Forecasting (ECMWF) model is one of the most sophisticated and computationally expensive operational numerical models currently used by the NHC. The ECMWF model provides forecasts up to 240 hours at 12-hour intervals daily (ECWMF 2019). In addition, the Hurricane Weather Research and Forecasting (HWRF) model provides forecast up to 126 hours every six hours (Biswas et al. 2018).

b. Statistical and Statistical-Dynamical Methods

Statistical approaches make predictions by modeling the historical relationships between storm-specific features, such as the time and location, and storm behavior. In comparison with dynamical models, statistical models are computationally more efficient, although predictions are

¹Multimodality in machine learning refers to the simultaneous use of different data formats, including, for example, tabular data, images, time series, free text, audio.

generally less accurate. Typically statistical models specialize in one of the forecasting tasks, either track or intensity.

The simplest form of a statistical model is a regression-based model. They are typically used as benchmarks to assess the modeling capabilities for more sophisticated methods. Some examples include the Climatology and Persistence Model (CLIPER5) (Abersson 1998) for track forecasts and the Statistical Hurricane Intensity Forecast (SHIFOR5) model for intensity forecasts only (Knaff et al. 2003).

In addition, statistical based models can employ predictive information obtained from dynamical models as input features, and hence they are called statistical-dynamical models. They can include rudimentary satellite-based information and use forecast fields from global models to infer future atmospheric and ocean surface conditions. Such models include the Statistical Hurricane Intensity Prediction Scheme (SHIPS) (DeMaria et al. 2005), improved as Decay-SHIPS to accommodate the transition of the TC to land.

Furthermore, recent advances in the machine learning community have been applied to improve statistical-based models. For instance, Moradi Kordmahalleh et al. (2016) and Alemany et al. (2019) have used Recurrent Neural Networks for track forecasting by modeling it as a time series problem. Chen et al. (2019), Lian et al. (2020) and Giffard-Roisin et al. (2020) have demonstrated the potential of Convolutional Neural Networks to process historical statistical data and satellite imagery data to make predictions.

c. Ensemble models

Typically, ensemble (consensus) forecasts are obtained by combining the forecasts from either multiple runs of a single model or a collection of individual models. Often, ensemble models can produce more accurate forecasts than individual ensemble members' predictions, as they combine the strengths of different approaches (Goerss 2000; Sampson et al. 2008).

For single-model ensembles, such as the U.S. National Weather Service Global Forecast System (GFS) mean ensemble (AEMN), multiple runs from one model are used to make multiple predictions, using different initial conditions to account for the uncertainties. On the other hand, multiple-model ensembles build forecasts based on the outputs of each ensemble member. Several models used by the NHC, such as the GUNS, GUNA, and CGUN models, use equally-weighted average among member models; whereas the Florida State University Super Ensemble (FSSE) model assigns different weights based on historical individual models' predicting power (Krishnamurti et al. 2011).

d. Relevant Machine Learning Techniques

1) NEURAL NETWORK-BASED MODELS

(i) *Recurrent Neural Networks* Recurrent Neural Networks are artificial neural networks that can model temporal dynamic behavior in time sequences. Their particular ability to recognize sequential characteristics and patterns in data makes them strong candidates for TC forecasting. In particular, the Long Short Term Memory (LSTM) (Hochreiter and Schmidhuber 1997) and Gated Recurrent Units (GRU) (Chung et al. 2014) are specifically designed to handle long-term dependencies in sequential problems. Several studies have demonstrated the use of RNNs to predict TC trajectory based on historical data (Moradi Kordmahalleh et al. 2016; Alemany et al. 2019; Gao et al. 2018).

(ii) *Convolutional Neural Networks* Convolutional neural networks (CNNs), a type of computer vision technique, have demonstrated impressive capabilities to analyze imagery data (LeCun et al. 1989; Krizhevsky et al. 2012; He et al. 2016). In particular, several studies demonstrate the potential of applying CNN-based architecture to process reanalysis data and satellite data for track forecasting (Giffard-Roisin et al. 2020; Lian et al. 2020; Mudigonda et al. 2017) and storm intensification forecasting (Chen et al. 2019; Su et al. 2020).

(iii) *Encoder-Decoder, Attention and Transformers* Encoder-Decoder neural network architectures became popular with the Natural Language Processing (NLP) field. Generally, the architecture consists of an encoder component, which transforms the input into a fixed shape embedding, and a decoder component, which transforms the embedding to a designated output.

In the context of sequential data, Attention Mechanisms (Bahdanau et al. 2015) have been introduced to improve the modeling capacity of sequence-to-sequence models for long-term dependencies. The general underlying principle of attention mechanisms is to learn the most relevant features to make a prediction by giving more or less attention (weight) to certain input components.

To leverage attention mechanisms, Vaswani et al. (2017) proposed the Transformer architecture which has gained significant traction in the Natural Language Processing (NLP) community (Devlin et al. 2018; Liu et al. 2019; Lan et al. 2019; Brown et al. 2020) due to superior modeling capacity and computational efficiency. In contrast with RNNs, Transformers process sequences as a whole instead of sequentially, thus improving the long term modeling power. Moreover, Yun et al. (2019) demonstrated the general expressive power of Transformers on sequence-to-sequence tasks, which motivates using such architectures for TC forecasting.

2) TENSOR DECOMPOSITION METHODS

A tensor is a multilinear array, generalizing vectors and matrices to higher dimensions. Therefore, tensor analysis offers a potent mathematical framework to analyze high dimensional data. In particular, tensor decomposition techniques are commonly used in the field of signal processing to compress and de-noise high dimensional data. The technique can be understood as performing high dimensional principal component analysis (Kolda and Bader 2009; Sidiropoulos et al. 2017). Specifically, Yan et al. (2014) shows such decomposition techniques can be applied to perform feature extraction tasks from imagery data, and Chen et al. (2018) show that a specific type of Tucker decomposition demonstrates capabilities to capture spatial-temporal relationships, thus motivating this work to explore using tensor decomposition as an unsupervised learning approach to perform feature extraction on high dimensional imagery data.

3) TREE-BASED METHODS

Tree-based algorithms are one of the best and mostly used supervised learning methods because of their capabilities to model non-linear relationships, often leading to superior performance than linear models. There are three main categories of tree-based models: decision trees (Breiman et al. 1984; Bertsimas and Dunn 2017, 2019), which are the foundation of all tree-based models; random forest (Breiman 2001), an ensemble method built upon many independent trees; gradient boosting trees (Friedman 2001), an ensemble built upon sequential trees. The latter two are popular choices for machine learning tasks, as they can reach high accuracy, stability and often offer decent interpretability. In our work, we applied XGBoost (Chen and Guestrin 2016), which belongs to the gradient boosted tree framework, for its training speed and superior performance on our data set compared to the other tree-based methods mentioned.

3. Data

For this study, we use three kinds of data dated since 1980: historical storm data, reanalysis maps, and operational forecasts data from the NHC. While more than 3000 TCs from 6 different basins were recorded since 1980, we only keep those that reach a speed of 34 kn at some time, i.e., are classified at least as a Tropical Storm on the Saffir-Simpson hurricane wind scale, and where more than 60 h of data are available after they reached the speed of 34 kn for the first time.

a. Historical Storm Data Set

We obtained historical storm data from the National Oceanic and Atmospheric Administration, through the post-season storm analysis dataset IBTrACS (Knapp et al.

2010). Among the available features, we have selected the time, the latitude, the longitude and the pressure at the center of the TC, the maximum sustained wind speed from the WMO agency (or from the regional agency when not available) for the current location, the distance-to-land, the translation speed of the TC, the direction of the TC (in degrees), the nature of the storm and the basin (North-Atlantic, Eastern Pacific, Western Pacific, etc). The feature choice is consistent with previous statistical forecasting approaches (DeMaria and Kaplan 1994; DeMaria et al. 2005; Giffard-Roisin et al. 2020). In this paper, we will refer to this data as *statistical data*.

b. Reanalysis Maps

Reanalysis maps are used extensively for atmospheric monitoring, climate research, and climate predictions. They provide a comprehensive record of how weather and climate evolve, based on dynamical aspects of the Earth systems, such as the air pressure, humidity, and wind speed. In our work, we use the extensive ERA-5 reanalysis data set developed by the ECWMF. It contains high spatial resolution reanalysis maps from 1979 to the present (ERA5 2017). ERA5 provides hourly estimates of a large number of atmospheric, land and oceanic climate variables. The data cover the Earth on a 30km grid and resolve the atmosphere using 137 levels from the surface up to a height of 80km.

We extracted ($25^\circ \times 25^\circ$) maps centered at the storm locations across time, given by the IBTrACS dataset described previously, of resolution $1^\circ \times 1^\circ$, i.e., each cell corresponds to one degree of latitude and longitude, offering a sufficient frame size to capture the entire storm. We obtained nine reanalysis maps for each TC time step, corresponding to three different features, geopotential z , u and v components of the winds, at three atmospheric altitudes, 225, 500, and 700hPa (see Figure 1). The three features' choice is motivated by the physical understanding that wind direction and geopotential differences highly determine the TC evolution. Furthermore, the three different atmospheric altitudes should capture part of the air movements at different troposphere levels, corresponding to low, mid and high clouds, since wind fields are the direct observations of the atmospheric flows. Section 8 proposes future work to use reanalysis maps from additional atmospheric altitudes (e.g., lower levels such as 825 and 850hPa) and additional features (e.g., sea-surface temperature, vertical wind shear, relative humidity).

c. Operational Forecast Models

The operational forecast data is obtained from the ATCF data set, maintained by the National Hurricane Center (NHC) (Sampson and Schrader 2000; National Hurricane Center 2021). The ATCF data contains historical forecasts for tropical cyclones and subtropical cyclones in the North

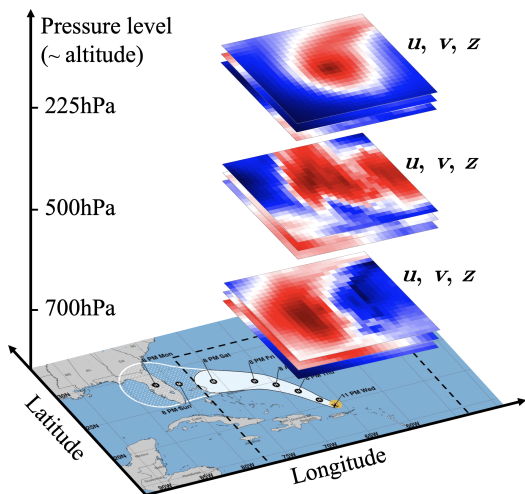


Fig. 1. Representation of the nine reanalysis maps extracted for each time step, corresponding to geopotential z , u and v components of the winds, repeatedly extracted at three atmospheric altitudes, 225, 500, and 700hPa. Each map is of size $25^\circ \times 25^\circ$, centered on the TC center location, and each pixel corresponds to the average field value at the given latitude and longitude degree.

Atlantic and Eastern Pacific basins, by operational models used by the NHC for its official forecasting. We select a subset of available operational models forecasts values (see detailed list in Table 2) as benchmarks for our experiments. The implementation of the forecast data extraction is done using the Tropycal Python package (Burg and Lillo 2020).

4. Problem Formulation

Our work aims to obtain accurate TC forecast with a machine learning approach utilizing a wide range of data, including historical storm-specific data and reanalysis data. To develop a spatial-temporal model that considers both the physical process and the statistical behavior, we identify three main challenges: 1) spatial (vision) data processing, 2) temporal data processing, 3) multimodality and data fusion. In the following subsections, we expand on each challenge and briefly outline our methodologies for addressing them. The precise methodology is further detailed in Section 5.

a. Challenge 1: Spatial Data Processing

Reanalysis maps give important information regarding the physical dynamics of the storm. Each map for one particular variable at a fixed time step and a fixed pressure level is a two-dimensional matrix, each axis corresponding to latitude and longitude. Then, as we use reanalysis maps at different pressure levels, the reanalysis feature maps form a three-dimensional tensor for each time step. Each pixel in the map thus corresponds to one of the variables at a given pressure level. Standard machine learning

algorithms such as tree-based models are not well-suited to take three-dimensional data as input. Hence, we embed spatial-temporal data into one-dimensional vectors using appropriate methodology. The principle is to obtain a compressed and predictive core representation of the 3-dimensional data. We call this process “feature extraction”.

In particular, we propose two different techniques to extract reanalysis maps embeddings: a supervised learning fashion with encoder-decoder network architectures (see 5.b.1) or an unsupervised fashion with tensor decomposition methods (see 5.b.2). The spatial-temporal features extracted can then be used along with statistical features to train standard machine learning algorithms.

b. Challenge 2: Temporal Data Processing

Temporal modeling of physical phenomena comes intrinsically with dynamical equations; however, the sequential modeling of time series data remains challenging for machine learning algorithms. In our models, for a specific prediction at a lead time of 24 h, we use a fixed sequence size of the past 21 h of corresponding TC data (i.e., 8 time steps spaced at a 3 h frequency). Then we can use recurrent neural networks or attention mechanisms with positional encoding (Vaswani et al. 2017) and sophisticated tree-based models like XGBoost to capture the nonlinear and temporal relationships between each time step of the sequence.

c. Challenge 3: Multimodality and Data Fusion

Multimodality in machine learning refers to the simultaneous use of different data formats, including, for example, tabular data, images, time series, free text, audio. As different modes represent different information channels, multiple sources are often semantically correlated and can provide complementary information to each other, unveiling invisible patterns when working with individual modalities and offering a richer potential for building new multimodal features. Using a wide range of data sources naturally leads to the question of data fusion. In particular, we need to build a framework that can process and make predictions based on data with different formats: from four-dimensional vision-based reanalysis maps to vectorized one-dimensional historical storm data consisting of numerical and categorical data.

The encoder-decoder neural network architecture is well-suited to deal with multimodal data as different kinds of neural network layers can be adapted to distinct modalities. We thus perform an intermediate fusion of the statistical data and vision data in the encoder, and the decoder handles the sequential aspect. Moreover, to further mix the features extracted by the encoder-decoder with the statistical data in a later stage, we demonstrate that a tree-based model can efficiently capture the complex nonlinear correlations and make meaningful predictions using each data

source. In summary, the statistical data is used twice: first to enhance the embedding process of the reanalysis maps by the encoder-decoder and second combined with the extracted embeddings and input in a gradient-boosted-tree model (see the pipeline in Figure 2).

5. Methodology

Overall, we adopt a three-step approach to combine distinct forecasting approaches and multiple data sources: first, we process each data source with relevant methodology. Second, we concatenate all the processed features in a one-dimensional format. Third, we make our predictions using a tree-based model trained on the selected data. At a given time step, we perform two 24-hour lead time forecasts: an intensity prediction task, i.e., predicting the intensity of the storm at a 24-hour lead time; a displacement regression task, i.e., predicting the latitude and longitude storm displacement in degrees between given time and forward 24-hour time. Figure 2 illustrates the three-step pipeline.

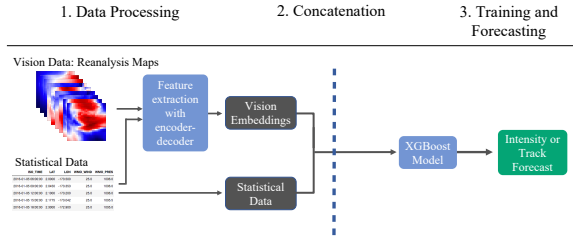


Fig. 2. Representation of our multimodal machine learning framework using the two data sources: statistical and reanalysis maps. During Step 1, data are processed individually to produce features using corresponding techniques. In particular we extract embeddings from the reanalysis maps using encoder-decoder architectures or tensor decomposition. See Section 5.a and 5.b for further details. During Step 2, we concatenate a combination of features. See Section 5.c for further details. During Step 3, we train one XGBoost model for each of the prediction tasks: intensity in 24 h, latitude displacement in 24 h, and longitude displacement in 24 h. See Section 5.d for further details.

We explore several combinations of data to determine the best model. We discuss our various techniques for processing statistical and vision data (reanalysis maps); then, we explain the technique for data fusion and finally make the prediction.

a. Statistical Data Processing

We process statistical data through several steps to engineer useful features for tree-based models.

First, categorical features are treated using the one-hot encoding technique. For a specific categorical feature, each possible category is converted as an additional feature, with 1 indicating the sample belongs to this category and 0 otherwise. We encode the basin and the nature of the TC as one-hot features.

Second, cyclical features are encoded using cosine and sine transformations to avoid singularities at endpoints. Features processed using this smoothing technique include date, latitude, longitude, and storm direction.

Third, missing values are treated using a linear interpolation method. Missing values concern maximum sustained wind speed and pressure features due to some discrepancies in 6-hour vs. 3-hour recording frequencies. For our model, we chose a 3-hour time step frequency to provide higher training granularity.

Finally, we engineer two additional features per time-step to capture first-order dynamical effects: the latitude and longitude displacements between two consecutive steps.

As a remark, the maximum sustained wind speed feature reported by the WMO agency can have different averaging policies depending on the basin, ranging from 1-minute to 10-minute intervals. In this work, we did not make explicit adjustments to account for such differences.

b. Vision Data Processing

We have experimented with two computer vision techniques to perform feature extraction from reanalysis maps: (1) encoder-decoder networks and (2) tensor decomposition methods. The former is a supervised learning method; for each input, there is an associated labeled value as a prediction target. We report in particular about two specific encoder-decoder architectures: a CNN-encoder GRU-decoder and a CNN-encoder Transformer-decoder. The latter is an unsupervised method; there is no specific labeled prediction target, and instead predictions are drawn directly from the patterns within the data.

1) ENCODER - DECODER ARCHITECTURES

We perform two successive tasks based on the encoder-decoder architectures: (i) directly predict TC intensity and track, (ii) once the network is trained, we fix its weights and extract low-dimensional reanalysis maps embeddings as features to be input into tree-based methods.

The CNN component acts as an encoder, and either a GRU or a Transformer component acts as a decoder. The CNN component aims to process (embed) the reanalysis maps. The GRU aims to model the temporal aspect through a recurrence mechanism, while the Transformer utilizes attention mechanisms and positional encoding to model long-range dependencies.

Figure 3 and 4 illustrate the encoder-decoder architectures. More details on all components are given in Appendix.

(i) *Predict TC intensity and track* To make a 24-hour lead time forecast, we use a fixed historical window size of past 21-hour data, corresponding to 8 distinct 3-hour frequency time steps in the data set.

The CNN-encoder At each time step, the corresponding nine reanalysis maps (see Section 3.b) are fed into the CNN-encoder, which produces one-dimensional embeddings. The CNN-encoder consists of three convolutional layers, with ReLU activation and MaxPool layers in between, then followed by two fully connected layers (see Appendix for exact architecture).

Next, we concatenate the reanalysis maps embeddings with processed statistical data corresponding to the same time step. Note that at this point data is still sequentially structured as 8 time steps to be passed on to the GRU-decoder or the Transformer-decoder.

The GRU-decoder Our GRU-decoder consists of two unidirectional layers. The data sequence embedded by the encoder is fed sequentially in chronological order into the GRU-decoder. For each time step, the GRU-decoder outputs a hidden state representing a “memory” of the previous time steps. Finally, a track or intensity prediction is made based upon these hidden states concatenated all together and given as input to fully-connected layers (see Figure 3).

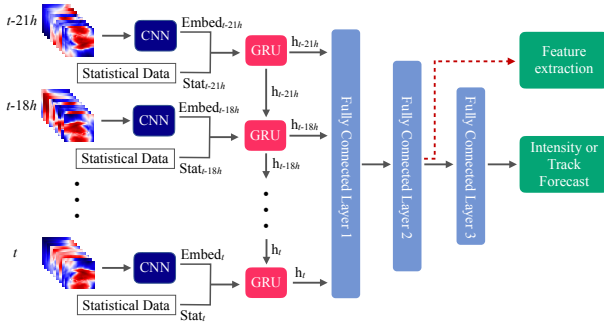


FIG. 3. Representation of our CNN-encoder GRU-decoder network for an 8-time step TC sequence. At each time step, we utilize the CNN to produce one-dimensional embeddings of the reanalysis maps. Then, we concatenate these embeddings with the corresponding statistical features to create a sequence of inputs fed sequentially to the GRU. At each time step, the GRU outputs a hidden state passed to the next time step. Finally, we concatenate all the successive hidden states and pass them through three fully connected layers to predict intensity or track with a 24-hour lead time. Spatial-temporal embeddings can be extracted as the output of the second fully connected layer.

The Transformer-decoder Conversely to the GRU-decoder, the sequence is fed as a whole into the Transformer-decoder. Since attention mechanisms allow each hidden representation to attend holistically to the other hidden representations, the time-sequential aspect is lost. Therefore, we add a *positional encoding* token at each timestep-input, following standard practices (Vaswani et al. 2017). This token represents the relative position of a time-step within the sequence and re-introduces some information about the inherent sequential aspect of the data

and experimentally improves performance (see Appendix for details).

Then, we use two Transformer layers that transform the 8 time steps (of size 142) into an 8-timestep sequence with similar dimensions. To obtain a unique representation of the sequence, we average the output sequence feature-wise into a one-dimensional vector, following standard practices. Finally, a track or intensity prediction is made based upon this averaged vector input into one fully-connected layer (see Figure 4).

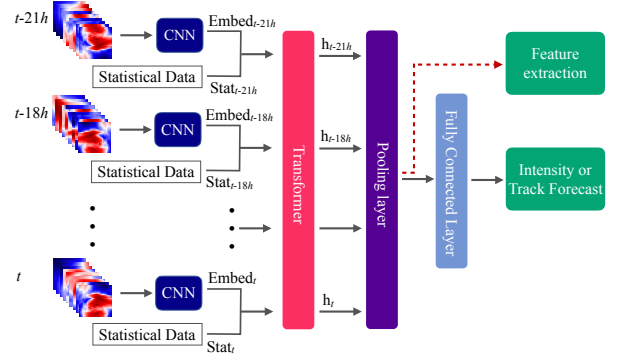


FIG. 4. Representation of our CNN-encoder Transformer-decoder network for an 8-time step TC sequence. At each time step, we utilize the CNN to produce one-dimensional embeddings of the reanalysis maps. Then, we concatenate these embeddings with the corresponding statistical features to create a sequence of inputs fed as a whole to the Transformer. The Transformer outputs a new 8-timestep sequence that we average (pool) feature-wise and then feed into one fully connected layer to predict intensity or track with a 24-hour lead time. Spatial-temporal embeddings can be extracted as the output of the pooling layer.

Training process We train the aforementioned encoder-decoder architectures in an end-to-end fashion, using standard backpropagation to update the weights parameterizing the model (Rumelhart et al. 1985; Goodfellow et al. 2016). We use a mean squared error loss with either an intensity or track objective and add an $L2$ regularization penalty on the network’s weights (see Appendix for further details).

(ii) *Feature extraction* In addition to directly forecasting TC intensity and track, the architecture provides predictive and low-size reanalysis maps’ embeddings.

After the training process described previously is completed, we freeze the encoder-decoder’s weights. Next, given an input sequence of reanalysis maps and statistical data, we pass them through the whole network, in the same fashion as before, except from the last fully-connected layer (see Figure 3 and 4). The second fully connected layer after the GRU or the pooling layer after the Transformer output a vector of relatively small size, e.g., 128 features, to compress information and provide more predictive features for our following tree-based methods. This vector constitutes our one-dimensional reanalysis maps embedding that we

extract from the initial 45,000 ($8 \times 9 \times 25 \times 25$) features, forming the spatial-temporal input.

The motivation is that while the encoder-decoder acquired intensity or track prediction skills during training, it captures relevant reanalysis maps embeddings. Using these internal features as input to an external model is a method inspired by transfer learning and distillation, generally efficient in visual imagery (Yosinski et al. 2014; Kiela and Bottou 2014; Tan et al. 2018; Hinton et al. 2015).

Comparison of our encoder-decoders with related work Giffard-Roisin et al. (2020) employed a similar CNN architecture for track forecast, using statistical data and reanalysis maps, but did not use any decoder component, and therefore did not account for the temporal aspects of the data. Besides, the intensity forecasting task was not explored in their work. Chen et al. (2020) used a hybrid CNN-LSTM network for hurricane formation and intensity forecasting but did not explore track forecasting nor augmented their models with statistical data. None of these two approaches explored feature extraction from neural networks, and to the best of our knowledge, our work is the first benchmark on this methodology for TC forecasting.

2) TENSOR DECOMPOSITION

In addition to a neural network approach, we explored tensor decomposition methods as a means of feature extraction. The motivation of using tensor decomposition is to represent high dimensional data using low dimension features. Throughout this work, we use the Tucker decomposition definition, which is also known as the higher order singular value decomposition. In contrast to aforementioned neural network-based feature processing techniques, tensor decomposition is an unsupervised extraction technique, which means features are not learned with respect to specific prediction targets. More details can be found in the Appendix.

At each time step, we treat past reanalysis maps over past time steps as a four-dimensional tensor, of size $8 \times 9 \times 25 \times 25$ (corresponding to 8 past time steps of 9 reanalysis maps of size 25 pixels by 25 pixels), and used the core tensor obtained from the Tucker decomposition as extracted features. The decomposition is achieved using the multilinear singular value decomposition (SVD) method, which is computationally efficient (De Lathauwer et al. 2000). Finally, the core tensor is flattened and can be concatenated with the corresponding statistical features to train tree-based methods. More details on tensor decomposition methodology can be found in the Appendix.

As a remark, the size of the core tensor, i.e., the Tucker rank of the decomposition, is a hyperparameter to be tuned. Based on validation, the Tucker rank is tuned to size $3 \times 5 \times 3 \times 3$ (see Section 6 for more details).

c. Concatenation

Various versions of the framework use different data sources as input data; as such, we concatenate features from relevant data sources to form a one-dimensional vector.

First, we concatenate the whole statistical data sequence corresponding to the fixed window size of past observations into a one-dimensional vector. As a result, the features' time-sequential aspect is no longer explicitly defined, and instead, we rely on sophisticated tree-based models to learn the complex non-linear dynamics. If the model's specific variation includes vision data, we concatenate the extracted one-dimensional vision data embeddings based on the particular processing technique (see Section 5). Finally, we perform feature-wise standardization on the concatenated data.

d. Summary of Models

In the scope of this work, we have experimented with various architectures based on different input data sources to make intensity and track forecasting. This section lists all the forecast models tested and retained and summarizes the methodologies employed during the processing and training stages in Table 1.

Model 1 and 2 utilize vision data (reanalysis maps) coupled with statistical data, employing neural networks only with the encoder-decoder architecture detailed in Section 5.b.1. Both models employ a CNN-encoder architecture, but Model 1 employs GRUs as decoder, while Model 2 employs Transformers.

Models 3-6 are variations of the three-step framework described in Figure 2, with the variation of input data source or processing technique. Model 3, HURR-(stat,xgb), has the simplest form, utilizing only statistical data. Model 4-6 utilize statistical data and vision data. They differ on the extraction technique used on the reanalysis maps. Model 4, HURR-(stat/viz,xgb/td), uses vision features extracted with tensor decomposition technique (see 5.b.2), whereas Model 5 and 6 utilize vision features extracted with the encoder-decoder (see 5.b.1), with GRU and Transformer decoders respectively.

Finally, Model 7 — HURR-consensus — and 8 — HURR/OP-average — are consensus models. Model 7 is a weighted consensus model of Models 1 to 6 forecasts. The weights given to each model are optimized using ElasticNet. As we trained multiple models using different data processing techniques and data sources, we built a diversified pool of predictors. This is typically the scenario where ensemble models can improve performance.

Model 8 is a simple average consensus of a few operational forecasts models used by the NHC and our Model 6, HURR-(stat/viz,xgb/cnn/transfo). We use Model 8 to explore whether the Hurricast framework can bring additional benefits to current operational forecasts by comparing its inclusion as a member model.

TABLE 1. Summary of the various versions of the Hurricast framework for which we report results. Models differ in architecture and in data used. The data used can be a subset of statistical, vision (reanalysis maps embedded or not), and operational forecasts. For this reason, models are named based on two characteristics: the data used and the methods used.

N°	Name	Data Used	ML Methods
1	HURR-(viz, cnn/gru)	Vision, Statistical	CNN, GRU
2	HURR-(viz, cnn/transfo)	Vision, Statistical	CNN, Transformers
3	HURR-(stat, xgb)	Statistical	XGBoost
4	HURR-(stat/viz, xgb/td)	Statistical, Vision embeddings	XGBoost, Tensor decomposition
5	HURR-(stat/viz, xgb/cnn/gru)	Statistical, Vision embeddings	XGBoost, CNN, GRU
6	HURR-(stat/viz, xgb/cnn/transfo)	Statistical, Vision embeddings	XGBoost, CNN, Transformers
7	HURR-consensus	Models 1-6 forecasts	ElasticNet
8	HURR/OP-average	Operational forecasts, HURR-(stat/viz, xgb/cnn/transfo)	Simple average

We provide further details on the performance of these different models compared to operational forecasts in the following Section 6.

6. Experiments

In this section, we first describe our metrics for evaluating the models. We then explain our training, validation, and testing protocols and finally give the best combinations of hyperparameters found.

a. Evaluation Metrics

We make two types of comparisons: (i) the standalone performance of our Hurricast models described in Table 1; (ii) the performance of operational forecasts consensus using or not Hurricast predictions.

To evaluate our intensity forecasts' accuracy, we compute the mean average error on the predicted 1-minute maximum sustained wind speed in 24 hours, as provided by the NHC for the North Atlantic and Eastern Pacific basins, defined as:

$$\text{MAE} := \frac{1}{N} \sum_{i=1}^N |y_i^{\text{true}} - y_i^{\text{pred}}|,$$

where N is the number of predictions, y_i^{pred} the predicted forecast intensity with a lead time of 24 h and y_i^{true} the ground-truth 1-min maximum sustained windspeed value given by the WMO agency.

To evaluate our track forecasts' accuracy, we compute the mean geographical distance error in kilometers between the actual position and the predicted position in 24 h, using the Haversine formula. The Haversine metric (see Appendix for the exact formula) calculates the great-circle distance between two points — i.e., the shortest distance between these two points over the Earth's surface.

b. Training, Validation and Testing Protocol

We now describe our model training, validation, and testing protocol. We use the train set to fit the model's weights on the data, the validation set to validate the hyperparameters choice, and the test set to provide an unbiased evaluation of the final trained model. We first explain how we split the data set and then describe the test set and testing methodology in more detail. Finally, we discuss the adjustments required to train the specific Hurricast model 7, HURR-consensus, that uses operational forecasts.

1) DATA SET SPLIT

We separate the data set into training (80% of the data), validation (10% of the data) and testing (10% of the data). The training set ranges from 1980 to 2011, the validation set from 2012 to 2015, and the test set from 2016 to 2019. Within each set, all samples are treated independently.

For models 1-6, we use data from all basins during training, but we only validate and test on the North Atlantic and Eastern Pacific basins, where we have benchmarks available.

2) DESCRIPTION OF THE TEST SET

The test set comprises all the TC time steps between 2016 and 2019 from the NA and EP basins where several operational forecast values are concurrently available, to be used as benchmarks to evaluate our models. In particular, we have selected the following operational forecasts as benchmarks based on availability and performance: Decay-SHIPS, GFSO, HWRF, FSSE and OFCL for the intensity forecast; CLP5, HWRF, GFSO, AEMN, FSSE and OFCL for the track forecast. We always compare all models on the same time steps. Table 2 summarises these models with their name and type.

TABLE 2. Summary of all operational forecast models included in our benchmark.

Model ID	Model name or type	Model type	Forecast
CLP5	CLIPER5 Climatology and Persistence	Statistical (baseline)	Track
Decay-SHIPS	Decay Statistical Hurricane Intensity Prediction Scheme	Statistical-dynamical	Intensity
GFSO	Global Forecast System model	Multi-layer global dynamical	Track, Intensity
HWRP	Hurricane Weather Research and Forecasting model	Multi-layer regional dynamical	Track, Intensity
AEMN	GFS Ensemble Mean Forecast	Consensus	Track
FSSE	Florida State Super Ensemble	Corrected consensus	Track, Intensity
OFCL	Official NHC Forecast	Consensus	Track, Intensity

3) TESTING METHODOLOGY

We employ the validation set to perform hyperparameter tuning, i.e., finding the best combination of hyperparameters. Then, using tuned hyperparameters, we retrain the models on the training and validation set combined. We then evaluate our models’ performance on the test set. For both intensity and track forecasts, we report the performance obtained on the NA and EP test set with each method, for 24-hour lead time forecasts. As a remark, in reality, there is often a time lag when operational models become available, and such lag is shorter for statistical models but longer for dynamical models (up to several hours) because of expensive computational time. Due to the lag time variability, we do not consider such lag in our comparisons with operational models, which is to our disadvantage since our forecasts compute in seconds. In other words, we neglect the time lag for all models and compare model results assuming all forecasts compute instantaneously. We hope to provide an overall sense of the predictive power of our methodology, which competes with operational forecasts even with disadvantages. However, we also acknowledge that using reanalysis maps data is not possible in real-time, and we discuss this bottleneck in section 8.

4) THE SPECIFIC PROTOCOL FOR HURR-CONSENSUS

For the HURR-consensus model, we use the HURR models 1-5 trained on the training set only (i.e., data until 2011). We then use their forecasts on the unseen validation set (2012 to 2015) and their forecasts on the unseen test set (2016 to 2019) as the training and testing data for the ensemble. The goal is to understand how each model behaves with respect to the others on unseen data. We cross-validate the ElasticNet parameters on the 2012-2015 HURR forecasts and we finally test on the same test years as before using the best hyperparameter combination found.

c. Hyperparameter Tuning

In this subsection, we provide the list of hyperparameters and the best configurations based on validation. We distinguish five categories of hyperparameters to tune: (1) the data-related features, (2) the neural-network related features, (3) the tensor decomposition-related features, (4) the tree-based method related features, (5) the consensus models-related features.

1) DATA RELATED FEATURES

The data-related features include the size of the reanalysis maps and the number of historical time steps of data to use for each forecast. We tune these features by comparing the 24-hour lead time forecast performance of the encoder-decoders for each different hyperparameter configuration.

We found that using eight past time steps (i.e., up to 21 h in the past) and a grid size of 25×25 degrees (in fact, the whole grid size we extracted initially) for the reanalysis maps was the best combination. We also found that standardizing the vision and statistical data — i.e., rescaling each feature to mean 0 and standard deviation 1 — yielded better results than normalizing — i.e., rescaling each feature to the $[0, 1]$ range.

2) NEURAL NETWORK-RELATED FEATURES

The neural network-related features include the optimizer, the architecture itself, the batch size during training, and the loss function’s regularizer. Recall that we have two downstream tasks for the neural network: an intensity regression task which consists of predicting the intensity of the storm in 24 h, and a displacement regression task which consists in predicting the latitude and longitude displacement of the storm in degrees between an instant t and $t + 24$ h.

The best results were obtained for both tasks using a batch size of 64, a λ regularization term of 0.01, and the encoder-decoder architectures described in the Appendix. Regarding the optimizer, we use Adam (Kingma and Ba

2014) with a learning rate of 10^{-3} for the intensity forecast and $4 \cdot 10^{-4}$ for the track forecast.

3) TENSOR DECOMPOSITION FEATURES

The tensor decomposition algorithm includes the choice of the core tensor size, i.e., the compressed size of the original tensor. Recall that the original tensor size is $8 \times 9 \times 25 \times 25$. Based on empirical testing, we found using a small tensor size of $3 \times 5 \times 3 \times 3$ yielded the best performance when compressed reanalysis maps are included as features in tree-based prediction methods.

4) TREE-BASED METHOD FEATURES

Based on empirical testing, we find XGBoost models consistently outperforming Decision Trees and Random Forests or other ML methods such as Support Vector Machines, regularized linear regression and multi-layer perceptrons. XGBoost trains also fast which is a considerable advantage for heavy hyperparameter search. Therefore, we select XGBoost as the core model for prediction. Then, there is variability in the best combinations of hyperparameters depending on each task (track or intensity), basin (NA or EP) or data sources to use (statistical, reanalysis maps embeddings, operational forecasts). However, these particular features were typically important and were the best in the following ranges: maximum depth of the trees (between 6 and 9), number of estimators (between 100 and 300), learning rate (between 0.03 and 0.15), subsample (between 0.6 and 0.9), column sampling by tree (between 0.7 and 1), minimum child by tree (between 1 and 5).

5) CONSENSUS-MODELS-RELATED FEATURES

We tested different kinds of ensemble models on the HURR forecasts, including ElasticNet (Zou and Hastie 2005), tree-based models, and multi-layer perceptrons (MLPs) as meta-learners. MLPs had similar performance with ElasticNet, but since they are less interpretable and stable, ElasticNet is the strongest ensembler candidate and our final choice. We tune the L1/L2 ratio between 0 and 1 and the regularization penalty between 10^{-4} and 10.

d. Computational Resources

All our code is in Python 3.6 (Van Rossum and Drake Jr 1995). Neural networks are coded using Pytorch (Paszke et al. 2019). We train all our models using one Tesla V100 GPU and 6 CPU cores. Typically, our encoder-decoders train within an hour, reaching the best validation performance after 30 epochs. One XGBoost model trains within two minutes. When doing a new prediction at test time, the whole model (encoder-decoder + XGBoost) runs within a couple of seconds, which shows practical interest for deployment. The bottleneck lies in the acquisition of

the reanalysis maps only. We further discuss this point in Section 8.a.

7. Results

(i) A multimodal approach leads to more accurate forecasts than using single data sources.

Under the scope of this work, we report six variations of the Hurricast framework (see Subsection 5.d for a summary of variations). The distinctions are based upon variations in data sources and variations in machine learning techniques, and we can group the variations into: 1) HURR-(stat,xgb) using only statistical data and tree-based models; 2) HURR-(viz, cnn/gru), HURR-(viz, cnn/transfo) using deep learning architectures only; 3) HURR-(stat/viz, xgb/cnn/gru), HURR-(stat/viz, xgb/cnn/transfo), HURR-(stat/viz, xgb/td) using statistical and vision data and tree-based models. The second and third categories of models use both statistical and vision data as input data, and hence are referred to as multimodal models.

As shown in Table 3 and Table 4, for both track and intensity forecasts, multimodal models achieve higher accuracy and lower standard deviation than the model using only statistical data.

Among multimodal approaches with feature extraction, deep-learning-based feature extraction approaches outperform the tensor-decomposition-based approach. It is not surprising as deep learning feature extraction uses a supervised learning objective, which means extracted features are tailored for the particular downstream prediction task, while tensor decomposition is advantageously label-agnostic.

Moreover, we show that extracting embeddings from encoder-decoder architectures is particularly useful and outperforms the standalone predictions made directly by the deep learning model. This suggests the additional value from using tree-based models that can combine efficiently diverse data sources. Therefore, our results show that multimodality with combining different machine learning techniques is a promising framework for TC forecasting. We experimentally show that useful embeddings can be extracted with adequate neural network architectures.

(ii) Standalone machine learning models can produce competitive results compared to operational models.

For intensity forecasting, as shown in Table 3, standalone Hurricast models outperform the most advanced statistical-dynamical model (Decay-SHIPS) and dynamical model (GFSO) in both NA and EP basins. Furthermore, our models produce competitive results with the most advanced dynamical model (HWRF). For track forecasting, as shown in Table 4, Hurricast models outperform the statistical benchmark model (CLP5), but underperform dynamical models (HWRF, GFSO).

These results highlight that machine learning approaches can emerge as a new methodology to currently

TABLE 3. Mean Average Error (MAE) and standard deviation of the error (Error sd) of standalone Hurricast models and operational forecasts on the same test set between 2016 and 2019, for intensity forecasting task.

Model Type	Model Name	Eastern Pacific Basin		North Atlantic Basin	
		Comparison on 36 TC		Comparison on 45 TC	
		MAE (kn)	Error sd (kn)	MAE (kn)	Error sd (kn)
Hurricast (HURR) Methods	HURR-(viz, cnn/gru)	10.7	10.1	11.4	9.6
	HURR-(viz, cnn/transfo)	10.5	10.0	11.4	9.5
	HURR-(stat, xgb)	10.5	10.4	10.8	9.3
	HURR-(stat, xgb/td)	10.6	10.4	10.5	9.1
	HURR-(stat/viz, xgb/cnn/gru)	10.3	10.1	10.8	9.3
	HURR-(stat/viz, xgb/cnn/transfo)	10.3	9.8	10.4	8.8
Standalone Operational Forecasts	Decay-SHIPS	11.7	10.4	10.2	9.3
	HWRF	10.6	11.0	9.7	9.0
	GFSO	15.7	14.7	14.2	14.1

TABLE 4. Mean Average Error (MAE) and standard deviation of the error (Error sd) of standalone Hurricast models and operational forecasts on the same test set between 2016 and 2019, for track forecasting task.

Model Type	Model Name	Eastern Pacific Basin		North Atlantic Basin	
		Comparison on 36 TC		Comparison on 45 TC	
		MAE (km)	Error sd (km)	MAE (km)	Error sd (km)
Hurricast (HURR) Methods	HURR-(viz, cnn/gru)	73	43	114	83
	HURR-(viz, cnn/transfo)	73	44	110	71
	HURR-(stat, xgb)	81	47	144	109
	HURR-(stat, xgb/td)	81	48	140	108
	HURR-(stat/viz, xgb/cnn/gru)	71	43	110	79
	HURR-(stat/viz, xgb/cnn/transfo)	72	43	110	72
Standalone Operational Forecasts	CLP5	121	67	201	149
	HWRF	67	42	75	49
	GFSO	65	45	71	54

existing forecasting methodologies in the field. In addition, we believe there is potential for improvement if given more available data sources.

(iii) *Our machine learning framework brings additional insights to consensus models.*

The NHC employs ensemble models to construct official forecasts, as they often produce better performance by averaging out errors from individual models. Hence, in this work, we include testings for two types of consensus models: the first type consists of weighting our individual Hurricast variations; the second type consists of a simple average of our best Hurricast variation and other standalone operational models.

As shown in Table 5 and Table 6, HURR-consensus, which is the weighted consensus of all individual Hurricast variations, consistently improves upon the best performing Hurricast variation, showcasing the possibility of building practical ensembles from machine learning models.

In addition, to validate whether a machine learning model can bring additional insights alongside current operational forecasts, we compare the accuracy of an average

consensus model with and without our model's inclusion. In particular, we use HURR-(stat/viz, xgb/cnn/transfo) model, which is generally the best performing variation of Hurricast models, alongside other standalone operational forecasts to form a consensus. We see that the version of consensus with the inclusion of Hurricast, i.e., HURR/OP-average consensus, is the best performing model, surpassing the NHC official forecast achieving higher accuracy with lower standard deviation for both track and intensity forecasting. These results suggest that the Hurricast model can bring additional insights into the consensus models, highlighting the complementary benefits of including a machine learning model. As discussed previously, we do not take into account the time lag for this experiment.

(iv) *Encoder-decoder standalone architectures produce competitive results with operational forecasting models.*

To the best of our knowledge, our encoder-decoder architectures combining both statistical data and vision data have been applied for the first time for TC track forecasting and reanalysis maps feature extraction. Results suggest

TABLE 5. Mean Average Error (MAE) and standard deviation of the error (Error sd) of consensus models compared with NHC’s official model OFCL on the same test set between 2016 and 2019 for intensity forecasting task.

Model Type	Model Name	Eastern Pacific Basin		North Atlantic Basin	
		Comparison on 36 TC		Comparison on 45 TC	
		MAE (kn)	Error sd (kn)	MAE (kn)	Error sd (kn)
Hurricast (HURR) Methods	HURR-(stat/viz, xgb/cnn/transfo)	10.3	9.8	10.4	8.8
	HURR-consensus	10.2	9.9	10.2	8.9
Operational Forecasts	FSSE	9.7	9.5	8.5	7.8
	OFCL	10.0	10.1	8.5	8.1
Consensus Models	Average consensus op. forecast	9.6	9.7	8.5	7.9
	HURR/OP-average consensus	9.2	9.0	8.3	7.6

TABLE 6. Mean Average Error (MAE) and standard deviation of the error (Error sd) of consensus models compared with NHC’s official model OFCL on the same test set between 2016 and 2019 for track forecasting task.

Model Type	Model Name	Eastern Pacific Basin		North Atlantic Basin	
		Comparison on 36 TC		Comparison on 45 TC	
		MAE (km)	Error sd (km)	MAE (km)	Error sd (km)
Hurricast (HURR) methods	HURR-(stat/viz, xgb/cnn/transfo)	72	43	110	72
	HURR-consensus	68	41	107	77
Operational Forecasts	AEMN	60	37	73	55
	FSSE	56	47	69	53
	OFCL	54	33	71	56
Consensus Models	Average consensus op. forecast	55	37	64	48
	HURR/OP-average consensus	50	32	61	43

these architectures are competitive with the best operational statistical-dynamical models for intensity forecasting. For track forecasting, the improvement over the CLP5 statistical baseline is significant but there are still limitations compared to the best operational forecasts, likely because the data itself is not predictive enough. The Transformer-decoder has sometimes a slight edge over the GRU-decoder, but both models are very performing.

8. Limitations and Extensions

This section discusses some limitations of our models and proposes approaches for future work.

a. Real-World Deployment

Currently, our models use reanalysis maps as input data. However, a significant limitation of using reanalysis maps is the computation time for construction, as they are assimilated based on observational data. Thus, although our models can compute forecasts in seconds, the dependence on reanalysis maps can be a bottleneck in real-time forecasting. Therefore, a natural extension for effective deployment is to train models using real-time observational data or available field forecasts from powerful dynamical models such as HWRF or GFS. Provided access to the relevant

data, we believe our framework still provides guidance and reference to build machine learning models to be deployed.

Furthermore, one can extend the framework to provide longer-term forecasts, such as 48-hour forecasts. We would consider training models using input data with longer past windows to obtain accurate longer-term forecasts.

b. Using Additional 3-Dimensional Features

Under the scope of this work, we used reanalysis maps corresponding to the geopotential, the u and v component of the wind fields from three altitude levels. One natural extension is to include information from more altitude levels, such as 825hPa and 850hPa, and additional features, such as the sea-surface temperature, the temperature, and the relative humidity, to increase the granularity of the data and hence improve the predictive power. In addition, the encoder-decoder architecture can be easily adopted to process other high-dimensional data, such as infrared and satellite imagery data. Our multimodal framework can easily incorporate new input data, and the new feature maps can be appended to pre-existing features to be included in the tree-based forecasting model. In particular, we propose two data fusion strategies: first, one can build a specialized feature extraction architecture per input data; second, one can fuse the input data before extracting features.

9. Conclusion

This study demonstrates a novel multimodal machine learning framework for tropical cyclone intensity and track forecasting utilizing three distinct data sources: historical storm data, reanalysis geographical maps, and operational forecasts. We present a three-step pipeline to combine multiple machine learning approaches, consisting of (1) data processing of individual data sets, (2) concatenation of all processed features, (3) prediction. We demonstrate that a successful combination of computer vision techniques and gradient-boosted trees can achieve strong predictions for both track and intensity forecasts, producing competitive results compared to current operational forecast models, especially in the intensity task.

We demonstrate that multimodal encoder-decoder architectures can successfully serve as a spatial-temporal feature extractor for downstream prediction tasks. In particular, this is also the first successful application of a Transformer-decoder architecture in tropical cyclone forecasting.

Furthermore, we show that ensemble models that include our machine learning model as an input can outperform the NHC's official forecast for both intensity and track, thus demonstrating the potential value of developing machine learning approaches as a new branch methodology for tropical cyclone forecasting.

Moreover, once trained, our models run in seconds, showing practical interest for real-time forecast, the bottleneck lying only in the reanalysis maps' acquisition. We propose extensions and guidance for effective real-world deployment.

In conclusion, our work demonstrates that machine learning can be a valuable approach to address bottlenecks in the field of tropical cyclone forecasting. We hope this work opens the door for further use of machine learning in meteorological forecasting.

Acknowledgments. We thank the review team of the Weather and Forecasting journal for insightful comments that improved the paper substantially. We thank Louis Maestrati, Charles Guille-Escuret, Baptiste Goujaud, David Yu-Tung Hui, Sophie Giffard-Roisin, Ding Wang, Tianxing He for useful discussions. We thank Nicolò Forcellini, Miya Wang for proof-reading. The work was partially supported from a grant to MIT by the OCP Group. The authors acknowledge the MIT SuperCloud and Lincoln Laboratory Supercomputing Center for providing high-performance computing resources that have contributed to the research results reported within this paper.

Data availability statement. All the data we used is open-source and can directly be accessed from the Internet with IBTrACS for TC features, Tropycal for operational forecasts, ERA-5 for vision data.

APPENDIX

Technical Components

a. Details on the CNN-Encoder GRU-Decoder Network

We provide more formal and precise explanations of our encoder-decoder architectures.

(i) *CNN-encoder GRU-decoder architecture details* Let t the instant when we want to make a 24-hour lead time prediction. Let $x_t^{\text{viz}} \in \mathbb{R}^{8 \times 9 \times 25 \times 25}$ be the corresponding spatial-temporal input of the CNN, where 8 is the number of past time steps in the sequence, 9 is the number of pressure levels times the number of features maps, $25^\circ \times 25^\circ$ is the pixel size of each reanalysis map. Let $x_t^{\text{stat}} \in \mathbb{R}^{8 \times 31}$ be the corresponding statistical data, where 8 is the number of time steps in the sequence, and 31 the number of features available at each time step.

First, x_t^{viz} is embedded by the CNN into $x_t^{\text{emb}} \in \mathbb{R}^{8 \times 128}$ where 8 is the number of time steps in the sequence, 128 is the dimension of the embedding space. Figure A1 provides an illustration of this embedding process by the CNN-encoder.

Let $i \in \{0, \dots, 7\}$ be the corresponding index of the time step in the sequence t . At each time step t_i of the sequence, the CNN embedding $x_{t_i}^{\text{emb}}$ is concatenated with the statistical data $x_{t_i}^{\text{stat}}$ and processed as

$$h_{t_i} := \text{GRU}(h_{t_{i-1}}, [x_{t_i}^{\text{emb}}, x_{t_i}^{\text{stat}}]),$$

with $h_{t_0} = \mathbf{0}$, $h_{t_i} \in \mathbb{R}^{128}, \forall i$. $[\cdot, \cdot]$ means concatenation of the two vectors along the column axis, to keep a one-dimensional vector.

Finally, we concatenate $h_{t_0}, h_{t_1}, \dots, h_{t_7}$ to obtain a one-dimensional vector x_t^{hidden} of size $8 \cdot 128 = 1024$ and pass this vector into a series of 3 fully connected linear layers, of input-output size: (1024, 512); (512, 128); (128, c), where $c = 2$ for track forecast task and $c = 1$ for intensity task. The final layer makes the prediction.

To extract the geospatial embedded features, we use the output of the second fully connected layer, of dimension 128. Therefore, this technique allows to reduce $8 \cdot 9 \cdot 25 \cdot 25 = 45,000$ features into 128 predictive features that can be input into our tree-based methods.

For each convolutional layer of the CNN, we use the following parameters: kernel size = 3, stride = 1, padding = 0. For each MaxPool layer, we use the following parameters: kernel size = 2, stride = 2, padding = 0.

The CNN-encoder architecture is largely inspired from Giffard-Roisin et al. (2020). The combination with the GRU-decoder or Transformer-decoder and the feature extraction is a contribution of our work.

b. Transformer-Decoder Architecture Details

As with the CNN-encoder GRU-decoder network, the spatial-temporal inputs are processed and concatenated

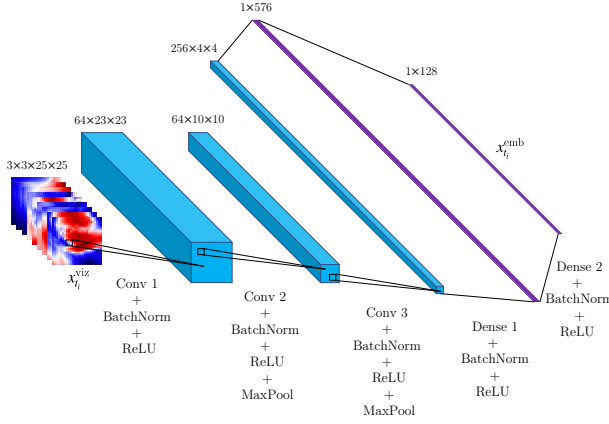


FIG. A1. Representation of our CNN-encoder. We use 3 convolutional layers, with batch normalization, ReLU and MaxPool in between. We use fully connected (dense) layers to obtain in the end a one-dimensional vector x_t^{emb} .

with the statistical data to obtain a sequence of input $[x_{t_i}^{emb}, x_{t_i}^{stat}]$, $\forall i \in \{0, \dots, 7\}$. As suggested by Vaswani et al. (2017), we add to each $[x_{t_i}^{emb}, x_{t_i}^{stat}]$ input a positional encoding P_i token in order to provide some information about the relative position i within the sequence. We eventually obtain $x = [x_{t_i}^{emb}, x_{t_i}^{stat}] + P_i$ which is being processed by the Transformer's layers. In this work, we use $P_{i,2j} = \sin(i/10000^{2j/d})$ and $P_{i,2j+1} = \cos(i/10000^{2j/d})$, where i is the position in the sequence, j the dimension and d the dimension of the model, in our case 142. A layer is composed of a Multi-Head attention transformation (explained below) followed by a Fully-connected layer, similar to the Transformer's encoder presented in Vaswani et al. (2017).

In this work, we use self-attention layers (i.e., $Q = K = V$), specifically 2 layers with 2 heads, the model's dimension d_k being fixed to 142 and the feedforward dimension set to 128.

The outputs of our Transformer $h_{t_0} \dots h_{t_T}$ are then averaged feature-wise to obtain the final representation of the sequence.

(i) *Loss function* The network is trained using an objective function \mathcal{L} based on a mean-squared-error loss on the variable of interest (maximum sustained wind speed or TC displacement) added to an $L2$ regularization term on the weights of the network:

$$\mathcal{L} := \frac{1}{N} \sum_{i=1}^N (y_i^{\text{true}} - y_i^{\text{pred}})^2 + \lambda \sum_l \sum_{k,j} W_{k,j}^{[l]2},$$

where N is the number of predictions, y_i^{pred} the predicted forecast intensity or latitude-longitude displacements with

a lead time of 24 h, y_i^{true} the ground-truth values, λ a regularization parameter chosen by validation, $W^{[l]}$ the weights of the l -th layer of the network. We minimize this loss function using the Adam optimizer (Kingma and Ba 2014).

c. Tucker decomposition for tensors

The multilinear singular value decomposition (SVD) expresses a tensor \mathcal{A} as a small core tensor \mathcal{S} multiplied by a set of unitary matrices. The size of the core tensor, denoted by $[k_1, \dots, k_N]$, defines the rank of the tensor. Formally, the multilinear decomposition can be expressed as:

$$\begin{aligned} \mathcal{A} &= \mathcal{S} \times_1 U^{(1)} \times_2 \dots \times_N U^{(N)} \\ \text{where } \mathcal{A} &\in \mathbb{R}^{I_1 \times I_2 \times \dots \times I_N} \\ \mathcal{S} &\in \mathbb{R}^{k_1 \times k_2 \times \dots \times k_N} \\ U^{(i)} &\in \mathbb{R}^{I_i \times k_i} \end{aligned}$$

where each $U^{(i)}$ is a unitary matrix, i.e., its conjugate transpose is its inverse $U^{(i)*} U^{(i)} = U^{(i)} U^{(i)*} = I$, and the mode- n product, denoted by $\mathcal{A} \times_n U$, denotes the multiplication operation of a tensor $\mathcal{A} \in \mathbb{R}^{I_1 \times I_2 \times \dots \times I_N}$ by a matrix $U \in \mathbb{R}^{I_n \times J_n}$. Figure A2 exhibits a geometric representation of the Tucker decomposition applied to a three-dimensional tensor \mathcal{A} , which is decomposed as a smaller core tensor \mathcal{S} and projection maps $U_{i=1,2,3}^i$.

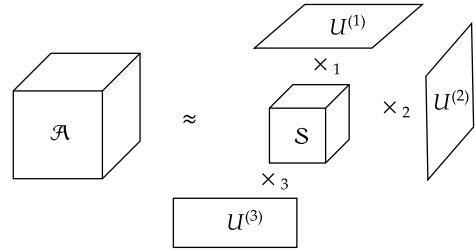


FIG. A2. Illustration of the tensor decomposition of a 3 dimensional tensor. Tensor \mathcal{A} is the original tensor, which is approximated through Tucker decomposition using a core tensor tensor \mathcal{S} and three linear projection maps along each axis $U^{(1)}, U^{(2)}, U^{(3)}$.

Analogous to truncated SVD, we can reduce the dimensionality of tensor \mathcal{A} by artificially truncating the core tensor \mathcal{S} and corresponding $U^{(i)}$. For instance, given a 4-dimensional tensor of TC maps, we can decide reduce the tensor to any desired rank by keeping only the desired size of core tensor \mathcal{S} . For instance, to reduce TC tensor data into rank $3 \times 5 \times 3 \times 3$, we first perform multilinear SVD, such that \mathcal{S} reflects descending order of the singular values, and then truncate \mathcal{S} by keeping only the first $3 \times 5 \times 3 \times 3$ entries, denoted by \mathcal{S}' , and the first 3 columns of each of $U^{(i)}$, denoted by $U'^{(i)}$.

Finally, we flatten the truncated core tensor \mathcal{S}' into a vector, which is treated as the extracted vision features in order to train tree-based model.

d. Haversine formula

Formally, the Haversine distance between one pair of predicted point and actual point, denoted by d , is calculated by:

$$d = 2R \arcsin(\sqrt{\alpha}), \text{ where}$$

$$\alpha = \sin^2\left(\frac{\hat{\phi} - \phi}{2}\right) + \cos(\hat{\phi}) \cos(\phi) \sin^2\left(\frac{\hat{\lambda} - \lambda}{2}\right)$$

where (ϕ, λ) are the actual latitude and longitude of one data point, $(\hat{\phi}, \hat{\lambda})$ are the predicted latitude and longitude, and R is Earth's radius, approximated to be the mean radius at 6,371 km.

References

- Aberson, S. D., 1998: Five-day tropical cyclone track forecasts in the north atlantic basin. *Weather and Forecasting*, **13** (4), 1005 – 1015.
- Aleman, S., J. Beltran, A. Perez, and S. Ganzfried, 2019: Predicting hurricane trajectories using a recurrent neural network. *Proceedings of the AAAI Conference on Artificial Intelligence*, Vol. 33, 468–475.
- Bahdanau, D., K. Cho, and Y. Bengio, 2015: Neural machine translation by jointly learning to align and translate. *CoRR*, **abs/1409.0473**.
- Bertsimas, D., and J. Dunn, 2017: Optimal classification trees. *Machine Learning*, **106** (7), 1039–1082.
- Bertsimas, D., and J. Dunn, 2019: *Machine learning under a modern optimization lens*. Dynamic Ideas LLC.
- Biswas, M. K., and Coauthors, 2018: Hurricane weather research and forecasting (hwrf) model: 2018 scientific documentation. *Developmental Testbed Center*.
- Breiman, L., 2001: Random forests. *Machine Learning*, **45** (1), 5–32.
- Breiman, L., J. H. Friedman, R. A. Olshen, and C. J. Stone, 1984: *Classification and Regression Trees*. Wadsworth and Brooks, Monterey, CA.
- Brown, T. B., and Coauthors, 2020: Language models are few-shot learners. *CoRR*, **abs/2005.14165**, 2005.14165.
- Burg, T., and S. P. Lillo, 2020: Tropycal: A python package for analyzing tropical cyclones and more. *34th Conference on Hurricanes and Tropical Meteorology*, AMS.
- Chen, R., X. Wang, W. Zhang, X. Zhu, A. Li, and C. Yang, 2019: A hybrid cnn-lstm model for typhoon formation forecasting. *Geoinformatica*.
- Chen, R., W. Zhang, and X. Wang, 2020: Machine learning in tropical cyclone forecast modeling: A review. *Atmosphere*, **11**, 676.
- Chen, T., and C. Guestrin, 2016: Xgboost: A scalable tree boosting system. *Proceedings of the 22nd ACM SIGKDD International Conference on Knowledge Discovery and Data Mining*, ACM, 785–794, KDD '16.
- Chen, X., Z. He, and J. Wang, 2018: Spatial-temporal traffic speed patterns discovery and incomplete data recovery via svd-combined tensor decomposition. *Transportation research part C: emerging technologies*, **86**, 59–77.
- Chung, J., Ç. Gülçehre, K. Cho, and Y. Bengio, 2014: Empirical evaluation of gated recurrent neural networks on sequence modeling. *CoRR*, **abs/1412.3555**, 1412.3555.
- De Lathauwer, L., B. De Moor, and J. Vandewalle, 2000: A multilinear singular value decomposition. *SIAM journal on Matrix Analysis and Applications*, **21** (4), 1253–1278.
- DeMaria, M., and J. Kaplan, 1994: A statistical hurricane intensity prediction scheme (ships) for the atlantic basin. *Weather and Forecasting*, **9** (2), 209–220.
- DeMaria, M., M. Mainelli, L. K. Shay, J. A. Knaff, and J. Kaplan, 2005: Further improvements to the statistical hurricane intensity prediction scheme (ships). *Weather and Forecasting*, **20** (4), 531 – 543.
- Devlin, J., M. Chang, K. Lee, and K. Toutanova, 2018: BERT: pre-training of deep bidirectional transformers for language understanding. *CoRR*, **abs/1810.04805**, 1810.04805.
- ECWMF, 2019: *PART III: Dynamics and Numerical Procedures*. No. 3, IFS Documentation, ECMWF, URL <https://www.ecmwf.int/node/19307>.
- ERA5, 2017: Era5 reanalysis. Research Data Archive at the National Center for Atmospheric Research, Computational and Information Systems Laboratory, Boulder CO, URL <https://doi.org/10.5065/D6X34W69>, accessed 2020-09-20.
- Friedman, J. H., 2001: Greedy function approximation: a gradient boosting machine. *Annals of statistics*, 1189–1232.
- Gao, S., P. Zhao, B. Pan, Y. Li, M. Zhou, J. Xu, S. Zhong, and Z. Shi, 2018: A nowcasting model for the prediction of typhoon tracks based on a long short term memory neural network. *Acta Oceanologica Sinica*, **37**, 8–12.
- Giffard-Roisin, S., M. Yang, G. Charpiat, C. Kumler Bonfanti, B. Kégl, and C. Monteleoni, 2020: Tropical cyclone track forecasting using fused deep learning from aligned reanalysis data. *Frontiers in Big Data*, **3**, 1.
- Goerss, J. S., 2000: Tropical cyclone track forecasts using an ensemble of dynamical models. *Monthly Weather Review*, **128** (4), 1187 – 1193.
- Goodfellow, I., Y. Bengio, and A. Courville, 2016: *Deep Learning*. The MIT Press.
- Grinsted, A., P. Ditlevsen, and J. H. Christensen, 2019: Normalized us hurricane damage estimates using area of total destruction, 1900–2018. *Proceedings of the National Academy of Sciences*, **116** (48), 23 942–23 946.
- He, K., X. Zhang, S. Ren, and J. Sun, 2016: Deep residual learning for image recognition. *Proceedings of the IEEE conference on computer vision and pattern recognition*, 770–778.
- Hinton, G., O. Vinyals, and J. Dean, 2015: Distilling the knowledge in a neural network. *NIPS Deep Learning and Representation Learning Workshop*.
- Hochreiter, S., and J. Schmidhuber, 1997: Long short-term memory. *Neural Comput.*, **9** (8), 1735–1780.

- Kiela, D., and L. Bottou, 2014: Learning image embeddings using convolutional neural networks for improved multi-modal semantics. *Proceedings of the 2014 Conference on Empirical Methods in Natural Language Processing (EMNLP)*, Association for Computational Linguistics, 36–45.
- Kingma, D., and J. Ba, 2014: Adam: A method for stochastic optimization. *International Conference on Learning Representations*.
- Knaff, J., M. DeMaria, C. Sampson, and J. Gross, 2003: Statistical 5-day tropical cyclone intensity forecasts derived from climatology and persistence. *Weather and Forecasting*, **18**, 80–92.
- Knapp, K. R., M. C. Kruk, D. H. Levinson, H. J. Diamond, and C. J. Neumann, 2010: The international best track archive for climate stewardship (ibtracs): Unifying tropical cyclone best track data. *Bulletin of the American Meteorological Society*, 91, 363–376.
- Knutson, T., and Coauthors, 2019: Tropical Cyclones and Climate Change Assessment: Part I: Detection and Attribution. *Bulletin of the American Meteorological Society*, **100** (10), 1987–2007.
- Kolda, T. G., and B. W. Bader, 2009: Tensor decompositions and applications. *SIAM review*, **51** (3), 455–500.
- Krishnamurti, T. N., M. K. Biswas, B. P. Mackey, R. G. Ellingson, and P. H. Ruscher, 2011: Hurricane forecasts using a suite of large-scale models. *Tellus A*, **63** (4), 727–745.
- Krizhevsky, A., I. Sutskever, and G. E. Hinton, 2012: Imagenet classification with deep convolutional neural networks. *Advances in neural information processing systems*, 1097–1105.
- Lan, Z., M. Chen, S. Goodman, K. Gimpel, P. Sharma, and R. Soricut, 2019: Albert: A lite bert for self-supervised learning of language representations. 1909.11942.
- LeCun, Y., B. Boser, J. S. Denker, D. Henderson, R. E. Howard, W. Hubbard, and L. D. Jackel, 1989: Backpropagation applied to handwritten zip code recognition. *Neural computation*, **1** (4), 541–551.
- Lian, J., P. Dong, Y. Zhang, J. Pan, and K. Liu, 2020: A novel data-driven tropical cyclone track prediction model based on cnn and gru with multi-dimensional feature selection. *IEEE Access*, **8**, 97 114–97 128.
- Lian, J., P. Dong, Y. Zhang, J. Pan, and K. Liu, 2020: A novel data-driven tropical cyclone track prediction model based on cnn and gru with multi-dimensional feature selection. *IEEE Access*.
- Liu, Y., and Coauthors, 2019: Roberta: A robustly optimized BERT pretraining approach. *CoRR*, **abs/1907.11692**.
- Moradi Kordmahalleh, M., M. Gorji Sefidmazgi, and A. Homaifar, 2016: A sparse recurrent neural network for trajectory prediction of atlantic hurricanes. *Proceedings of the Genetic and Evolutionary Computation Conference 2016*, 957–964.
- Mudigonda, M., and Coauthors, 2017: Segmenting and tracking extreme climate events using neural networks.
- National Hurricane Center, 2021: Automated tropical cyclone forecasting system (atcf). National Hurricane Center (NHC), URL <https://ftp.nhc.noaa.gov/atcf/>, accessed: 2021-04-06.
- Paszke, A., and Coauthors, 2019: Pytorch: An imperative style, high-performance deep learning library. *Advances in Neural Information Processing Systems 32*, H. Wallach, H. Larochelle, A. Beygelzimer, F. d'Alché-Buc, E. Fox, and R. Garnett, Eds., Curran Associates, Inc., 8024–8035.
- Rheme, J. R., 2007: Technical summary of the national hurricane center track and intensity models. *Updated September*, **12**, 2007.
- Rumelhart, D. E., G. E. Hinton, and R. J. Williams, 1985: Learning internal representations by error propagation. Tech. rep., California Univ San Diego La Jolla Inst for Cognitive Science.
- Sampson, C., and A. J. Schrader, 2000: The automated tropical cyclone forecasting system (version 3.2). *Bulletin of the American Meteorological Society*, **81**, 1231–1240.
- Sampson, C. R., J. L. Franklin, J. A. Knaff, and M. DeMaria, 2008: Experiments with a simple tropical cyclone intensity consensus. *Weather and Forecasting*, **23** (2), 304–312.
- Sidiropoulos, N. D., L. De Lathauwer, X. Fu, K. Huang, E. E. Papalexakis, and C. Faloutsos, 2017: Tensor decomposition for signal processing and machine learning. *IEEE Transactions on Signal Processing*, **65** (13), 3551–3582.
- Su, H., L. Wu, J. H. Jiang, R. Pai, A. Liu, A. J. Zhai, P. Tavallali, and M. DeMaria, 2020: Applying satellite observations of tropical cyclone internal structures to rapid intensification forecast with machine learning. *Geophysical Research Letters*, **47** (17).
- Tan, C., F. Sun, T. Kong, W. Zhang, C. Yang, and C. Liu, 2018: A survey on deep transfer learning. *CoRR*, **abs/1808.01974**, 1808.01974.
- Van Rossum, G., and F. L. Drake Jr, 1995: *Python tutorial*. Centrum voor Wiskunde en Informatica Amsterdam, The Netherlands.
- Vaswani, A., N. Shazeer, N. Parmar, J. Uszkoreit, L. Jones, A. N. Gomez, L. u. Kaiser, and I. Polosukhin, 2017: Attention is all you need. *Advances in Neural Information Processing Systems 30*, 5998–6008.
- Yan, H., K. Paynabar, and J. Shi, 2014: Image-based process monitoring using low-rank tensor decomposition. *IEEE Transactions on Automation Science and Engineering*, **12** (1), 216–227.
- Yosinski, J., J. Clune, Y. Bengio, and H. Lipson, 2014: How transferable are features in deep neural networks? *CoRR*, **abs/1411.1792**.
- Yun, C., S. Bhojanapalli, A. S. Rawat, S. J. Reddi, and S. Kumar, 2019: Are transformers universal approximators of sequence-to-sequence functions? *CoRR*, **abs/1912.10077**.
- Zou, H., and T. Hastie, 2005: Regularization and variable selection via the elastic net. *Journal of the Royal Statistical Society, Series B*, **67**, 301–320.